

# UC Davis

## UC Davis Previously Published Works

### Title

Mitochondrial dysfunction in brain tissues and Extracellular Vesicles Fragile X-associated tremor/ataxia syndrome.

### Permalink

<https://escholarship.org/uc/item/0zt5q1rt>

### Journal

Annals of Clinical and Translational Neurology, 11(6)

### Authors

Yao, Pamela

Manolopoulos, Apostolos

Eren, Erden

et al.

### Publication Date

2024-06-01


### DOI

10.1002/acn3.52040

Peer reviewed

## RESEARCH ARTICLE

# Mitochondrial dysfunction in brain tissues and Extracellular Vesicles Fragile X-associated tremor/ataxia syndrome

Pamela J. Yao<sup>1</sup>, Apostolos Manolopoulos<sup>1</sup> , Erden Eren<sup>1</sup>, Susan Michelle Rivera<sup>2,3</sup>, David R. Hessl<sup>3,4</sup>, Randi Hagerman<sup>3,5</sup>, Veronica Martinez-Cerdeno<sup>3,6,7</sup>, Flora Tassone<sup>3,8,\*</sup> & Dimitrios Kapogiannis<sup>1,\*</sup>

<sup>1</sup>Laboratory of Clinical Investigation, Intramural Research Program, National Institute on Aging, National Institutes of Health, Baltimore, Maryland, USA

<sup>2</sup>Department of Psychology, University of Maryland, College Park, Maryland, USA

<sup>3</sup>MIND Institute, University of California, Davis, Medical Center, Sacramento, California, USA

<sup>4</sup>Department of Psychiatry and Behavioral Sciences, University of California, Davis, School of Medicine, Sacramento, California, USA

<sup>5</sup>Department of Pediatrics, University of California, Davis, School of Medicine, Sacramento, California, USA

<sup>6</sup>Department of Pathology and Laboratory Medicine, University of California, Davis, School of Medicine, Sacramento, California, USA

<sup>7</sup>Institute for Pediatric Regenerative Medicine at Shriners Hospitals for Children Northern California, Sacramento, California, USA

<sup>8</sup>Department of Biochemistry and Molecular Medicine, University of California, Davis, School of Medicine, Sacramento, California, USA

## Correspondence

Flora Tassone, MIND Institute – Bioscience Building, Sacramento Campus, Sacramento, CA 95817, USA. Tel: +1 916 703 0463; Fax: +1 916 703 0367. E-mail: [ftassone@ucdavis.edu](mailto:ftassone@ucdavis.edu)

Dimitrios Kapogiannis, Laboratory of Clinical Investigation, Intramural Research Program, National Institute on Aging, National Institutes of Health, 3001 S. Hanover St., 5th floor/NIA, Baltimore, MD 21225, USA. Tel: +1 410 350 3953; Fax: +1 410 350 7308. E-mail: [kapogiannisd@mail.nih.gov](mailto:kapogiannisd@mail.nih.gov)

Received: 17 November 2023; Revised: 30 January 2024; Accepted: 24 February 2024

*Annals of Clinical and Translational Neurology* 2024; 11(6): 1420–1429

doi: 10.1002/acn3.52040

\*These authors share senior and corresponding authorships.

## Introduction

Fragile X-associated tremor/ataxia syndrome (FXTAS) is a late-onset neurodegenerative disorder characterized by a range of clinical manifestations including intention tremor, cerebellar ataxia, parkinsonism, and cognitive deficits.<sup>1–4</sup> FXTAS results from the presence of a CGG

## Abstract

**Objective:** Mitochondrial impairments have been implicated in the pathogenesis of Fragile X-associated tremor/ataxia syndrome (FXTAS) based on analysis of mitochondria in peripheral tissues and cultured cells. We sought to assess whether mitochondrial abnormalities present in postmortem brain tissues of patients with FXTAS are also present in plasma neuron-derived extracellular vesicles (NDEVs) from living carriers of fragile X messenger ribonucleoprotein1 (*FMRI*) gene premutations at an early asymptomatic stage of the disease continuum. **Methods:** We utilized postmortem frozen cerebellar and frontal cortex samples from a cohort of eight patients with FXTAS and nine controls and measured the quantity and activity of the mitochondrial proteins complex IV and complex V. In addition, we evaluated the same measures in isolated plasma NDEVs by selective immunoaffinity capture targeting LICAM from a separate cohort of eight *FMRI* premutation carriers and four age-matched controls. **Results:** Lower complex IV and V quantity and activity were observed in the cerebellum of FXTAS patients compared to controls, without any differences in total mitochondrial content. No patient-control differences were observed in the frontal cortex. In NDEVs, *FMRI* premutation carriers compared to controls had lower activity of Complex IV and Complex V, but higher Complex V quantity. **Interpretation:** Quantitative and functional abnormalities in mitochondrial electron transport chain complexes IV and V seen in the cerebellum of patients with FXTAS are also manifest in plasma NDEVs of *FMRI* premutation carriers. Plasma NDEVs may provide further insights into mitochondrial pathologies in this syndrome and could potentially lead to the development of biomarkers for predicting symptomatic FXTAS among premutation carriers and disease monitoring.

expanded allele in the premutation (PM) range (55–200 repeats) of the fragile X messenger ribonucleoprotein 1 (*FMRI*) gene<sup>5,6</sup>; by contrast, Fragile X syndrome (FXS) is associated with greater than 200 CGG repeats.

Neuropathologically, one distinctive feature of FXTAS is the accumulation of eosinophilic ubiquitin-positive intranuclear inclusions in neurons and astrocytes,

particularly, of the cerebellar nuclei, frontal cortex, and hippocampus.<sup>7–9</sup> In addition, a decrease in some mitochondrial proteins in FXTAS brain samples has been reported, which appeared to precede the accumulation of intranuclear inclusions,<sup>10</sup> thus, implying that mitochondrial defects may be an early event in the course of the disease. Subsequent studies using various sample types, from postmortem brains to blood cells or skin-derived fibroblasts, have further indicated that defective mitochondria, specifically impaired mitochondrial oxidative phosphorylation system, may contribute to FXTAS pathogenesis. Blood and fibroblast samples have been useful because changes in mitochondria can be examined in living *FMR1* PM carriers at different disease stages, even before progressing to FXTAS.<sup>11–15</sup> These studies have substantiated the link between mitochondrial defects and FXTAS pathogenesis; however, analysis of mitochondria in peripheral tissues may not directly reflect the brain's mitochondrial status.

Extracellular vesicles (EVs) are nanosized membranous particles that are released by all cell types. Their cargo comprises nucleic acids, lipids, and proteins, including mitochondrial components, that reflect the parental cell identity and homeostatic status.<sup>16</sup> EVs secreted by brain cells can cross the blood–brain barrier and be detected in blood, thereby providing a window into the brain.<sup>17</sup> We and others have isolated neuron-derived EVs (NDEVs) from patients' plasma<sup>18–21</sup> and have shown that NDEVs can be used as potential sources of biomarkers for various neurological disorders.<sup>21–23</sup>

The aim of this study was to investigate if mitochondrial dysfunction in FXTAS can be reflected in NDEVs. Studies of *FMR1* PM carriers and FXTAS patients have long hinted at abnormal mitochondrial oxidative phosphorylation that may contribute to the disease pathologies.<sup>10,13,24</sup> We measured the activity and quantity of mitochondrial respiratory complexes IV and V in post-mortem frozen brain tissues from patients with FXTAS, and also quantified the same measures in NDEVs isolated from the plasma of living *FMR1* PM carriers, similar to NDEV studies in other cohorts.<sup>19,20,25,26</sup>

## Methods

### Experimental design and study cohorts

We utilized a cohort of eight end-stage (Stage 4–5) patients with FXTAS and nine matched male controls, who had donated their brains to the University of California, Davis, School of Medicine, Sacramento, CA and were stored at the UC Davis FXTAS/FXS brain repository (Table 1).<sup>27</sup> Tissues of frontal cortex and cerebellum were chemically fixated and stored at  $-80^{\circ}\text{C}$ .

**Table 1.** Cohort characteristics for study of brain tissues.

Characteristic	Patients with FXTAS (N = 8)	Controls (N = 9)
Sex – no. (%)		
Female	0 (0.0)	0 (0.0)
Male	8 (100.0)	9 (100.0)
Age – years, mean (SD)	74.9 (5.9)	65.3 (8.5)
Tissue sample – no. (%)		
Frontal cortex	8 (100.0)	7 (77.8)
Cerebellum	8 (100.0)	9 (100.0)
FXTAS Stage – no. (%)		
1	0 (0.0)	
2	0 (0.0)	
3	0 (0.0)	
4–5	8 (100.0)	
6	0 (0.0)	

FXTAS, Fragile X-associated tremor/ataxia syndrome; SD, standard deviation.

For the study of NDEVs, a separate cohort of eight *FMR1* PM carriers, who had donated blood, was identified retrospectively at the University of California, Davis, School of Medicine, Sacramento, CA. Each individual had undergone a detailed clinical and genetic assessment and was given a diagnosis of early-stage (Stage 1–3) FXTAS according to diagnostic criteria.<sup>28,29</sup> Four additional male subjects, matched for demographic characteristics, who had also donated blood, were chosen as controls (Table 2). Blood samples were collected in EDTA tubes and, after centrifugation, 0.5 mL of plasma was stored at  $-80^{\circ}\text{C}$  and used for NDEV isolation and analysis.

The study and all protocols were carried out in accordance with the Institutional Review Board at the University of California, Davis. All participants gave written informed consent before participating in the study in line with the Declaration of Helsinki.

**Table 2.** Cohort characteristics for study of NDEVs.

Characteristic	<i>FMR1</i> PM carriers (N = 8)	Controls (N = 4)
Sex – no. (%)		
Female	1 (12.5)	0 (0.0)
Male	7 (87.5)	4 (100.0)
FXTAS Stage – no. (%)		
1	1 (8.0)	
2	3 (25.0)	
3	3 (25.0)	
4	1 (8.0)	
5	0 (0.0)	
6	0 (0.0)	

*FMR1* PM, fragile X messenger ribonucleoprotein 1 premutation; FXTAS, Fragile X-associated tremor/ataxia syndrome; NDEVs, neuron-derived extracellular vesicles.

## NDEV isolation

EDTA plasma aliquots were received and processed blindly by investigators at the National Institute on Aging, Baltimore, MD. NDEVs were isolated by immunoaffinity capture targeting L1 cell adhesion molecule (L1CAM), a transmembrane neuronal protein sorted to EVs, as previously described.<sup>18,21</sup> Briefly, 250  $\mu$ L of plasma was defibrinated with 100  $\mu$ L of thrombin followed by addition of 150  $\mu$ L of Dulbecco's PBS-1X (DPBS), supplemented with protease/phosphatase inhibitors, and sedimented at 3000g for 15 min at room temperature (RT). The supernatant was transferred to a sterile 1.5 mL microtube, and particles were sedimented by incubation with 126  $\mu$ L of ExoQuick<sup>TM</sup> followed by centrifugation at 1500g for 30 min at RT. Pelleted crude total EVs were resuspended by overnight gentle rotation mixing at 4°C in 350  $\mu$ L of ultra-pure distilled water supplemented with protease/phosphatase inhibitors. Resuspended crude total EVs were, then, incubated for 30 min at RT with 4  $\mu$ g of biotinylated anti-human L1CAM antibody. EV-antibody complexes were incubated with 25  $\mu$ L of washed Pierce<sup>TM</sup> Streptavidin Plus UltraLink<sup>TM</sup> Resin for 30 min at RT. After centrifugation at 600g for 10 min at 4°C and removal of unbound EVs and soluble proteins in the supernatant, NDEVs were eluted with 100  $\mu$ L of 0.1 M glycine, followed promptly by pH normalization. Beads were sedimented by centrifugation at 4000g for 10 min at 4°C, and supernatant containing immunoprecipitated NDEVs was collected. 10  $\mu$ L of intact NDEVs were stored at -80°C and used for determination of their diameter and concentration with nanoparticle tracking analysis (NTA) (Nanosight NS500 equipped with a 532 nm laser module; Malvern, Amesbury, UK), based on the Brownian motion of particles detected by light scattering. The remaining volume of NDEV preparations was used for downstream mitochondrial assays.

## Mitochondrial complex IV measurement

We measured mitochondrial complex IV in postmortem frontal cortex and cerebellum tissues and NDEVs using a human complex IV microplate (ab109910, Abcam plc, Cambridge, UK). In this assay, Complex IV was immunocaptured in the wells of an assay plate; its catalytic activity was determined colorimetrically based on the oxidation of reduced cytochrome c, and its quantity was then measured by ELISA in the same sample wells. The ratio of the activity and quantity represents the specific activity of Complex IV. For simplification, the term "activity" is used and refers to specific activity throughout the manuscript.

We carried out the assay following the manufacturer's instructions. For brain tissues, we homogenized the

samples in the assay buffer, added the detergent (provided in the assay kit, 10% final concentration), centrifuged the samples, collected the supernatants, and measured the protein concentration using the bicinchoninic acid (BCA) assay. The tissue samples containing 20  $\mu$ g of total protein were added to the wells of the assay plate. For NDEV samples, we lysed intact NDEVs in the assay buffer containing 10% detergent on ice for 30 min before loading the samples on the assay plate. The plate containing either brain tissue or NDEV samples was incubated overnight with gentle rocking at 4°C followed by measurement of Complex IV activity, quantity, and specific activity. All samples were run in duplicate.

## Mitochondrial complex V measurement

We measured Complex V in postmortem frontal cortex and cerebellum tissues and NDEVs using a human complex V microplate assay (ab109716, Abcam plc, Cambridge, UK). In this assay, Complex V is immunocaptured in the wells of an assay plate; its catalytic activity is determined colorimetrically based on the conversion of NADH to NAD<sup>+</sup>, and its quantity in the same sample wells is then measured by ELISA. The ratio of the activity and quantity represents the specific activity of complex V. Similarly to complex IV, the term "activity" was used to describe this ratio throughout the manuscript.

We carried out the assay following the manufacturer's instructions with minor modifications. For brain tissues, we homogenized the samples in the assay buffer, added the detergent (provided in the assay kit, 10% final concentration), and incubated on ice for 10 min. We then centrifuged the samples, collected the supernatants, and measured the protein concentration using the BCA assay. The tissue samples containing 20  $\mu$ g of total protein were added to the wells of the assay plate. For NDEV samples, we lysed intact NDEVs in the assay buffer containing 10% detergent on ice for 15 min before loading the samples on the assay plate. The plate containing either brain tissue or NDEV samples was incubated overnight with gentle rocking at 4°C followed by measurement of Complex V activity, quantity, and specific activity. All samples were run in duplicate.

## Mitochondrial content measurement

We used two methods to determine mitochondrial contents in the brain tissue homogenates: a mitochondrial membrane-specific dye MitoTracker Deep Red (MTDR)<sup>30,31</sup> and immunoblotting of mitochondrial citrate synthase, a mitochondrial matrix protein.

We carried out the MTDR method following the protocol described by Osto *et al.*<sup>32</sup> We homogenized the

brain tissues in cold MAS assay buffer and measured protein concentration with the BCA protein assay. Our pilot analysis revealed a linear correlation between MTDR fluorescence and protein amounts in the range of 2–20  $\mu\text{g}$  from the tissue homogenates. Therefore, we loaded the homogenates containing 20  $\mu\text{g}$  protein to each well of a clear flat-bottom black 96-well plate and added MTDR at 1  $\mu\text{M}$  final concentration. The plate was incubated at 37°C for 10 min and was centrifuged at 2000g for 5 min at 4°C. After removing unbound MTDR dye, 100  $\mu\text{L}$  MAS buffer was added and then removed gently from the assay wells. After adding another 100  $\mu\text{L}$  of MAS buffer, fluorescence was measured using a plate reader. All samples were run in quadruplicate.

Immunoblots of citrate synthase were carried out using the standard protocol for electrophoresis and immunoblotting. Briefly, equal protein amounts (20  $\mu\text{g}$ ) from the cerebellum tissues of seven patients with FXTAS and seven controls were separated by electrophoresis and immunoblotted with antibodies against citrate synthase (1:1000) (#14309, Cell Signaling Technology Inc., Danvers, MA) or actin (1:2500) (#A5441, MilliporeSigma, Burlington, MA). The proteins were visualized using a chemiluminescence kit (Pierce Biotechnology Inc., Waltham, MA). The intensity of protein bands was analyzed using ImageJ software.

### Oxygen consumption rate (OCR) measurement

To better understand the mitochondrial oxidative phosphorylation machinery in the brains of patients with FXTAS, we examined mitochondrial respiration using a protocol designed specifically for analyzing electron transport chain activity in frozen tissues.<sup>31–33</sup> In this protocol, providing chemicals (as electron donors) directly to the electron transport chain circumvents the components that are lost due to freezing and thawing, thereby enabling assessments of electron transport chain activity in the form of oxygen consumption rate (OCR). In this study, we focused on Complex I- and Complex II-mediated

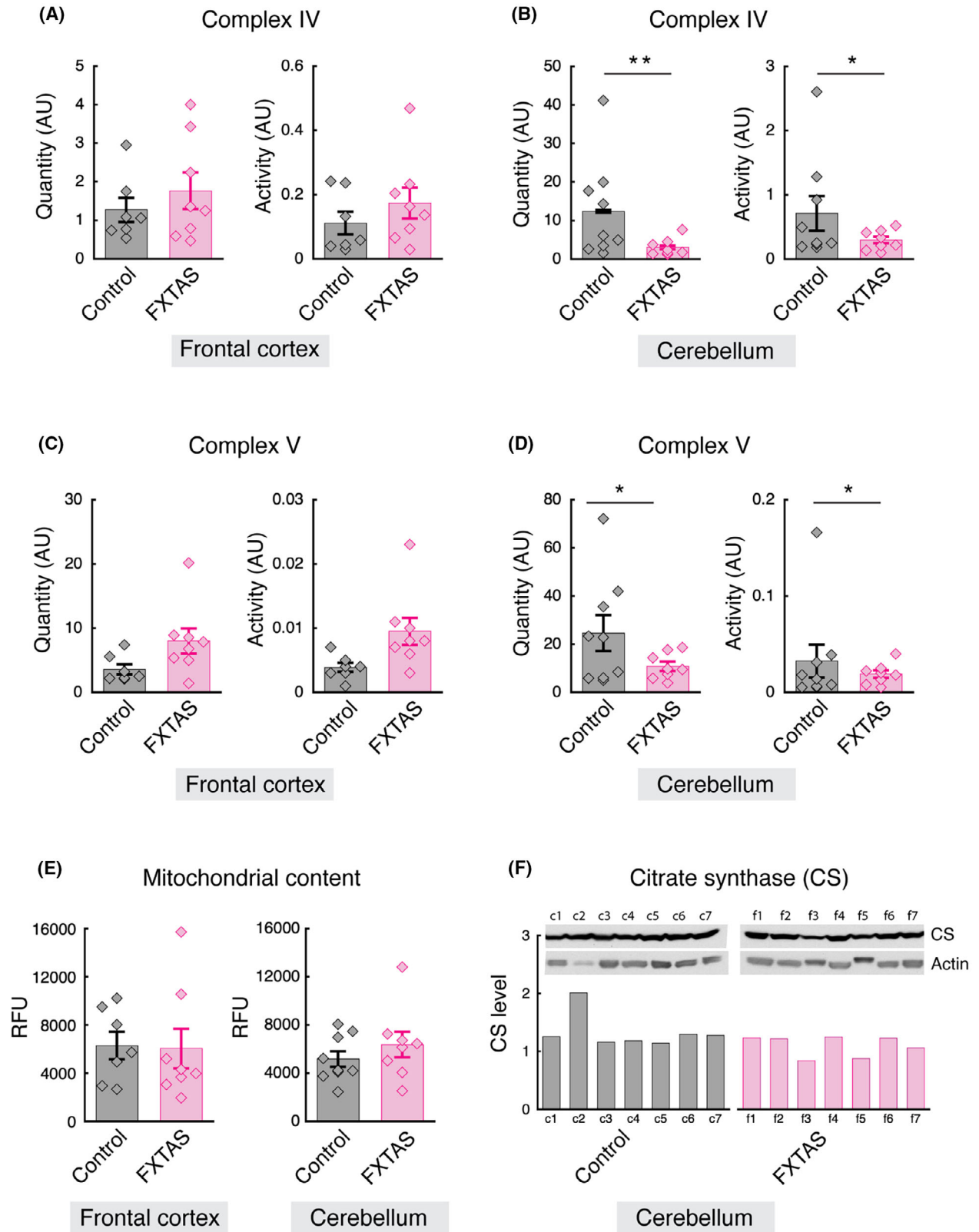
OCR by providing NADH (Fig. 2A) and succinate (Fig. 2C), respectively, to the tested tissue homogenates.

After rapidly thawing on ice, brain tissues were homogenized in cold MAS assay buffer, centrifuged at 1000g for 5 min at 4°C, and protein concentration of the supernatants was determined using the BCA protein assay. The samples containing 20  $\mu\text{g}$  of total protein in 20  $\mu\text{L}$  of the MAS buffer were loaded to each well of a Seahorse XF24 cell plate (Agilent Technologies, Inc., Santa Clara, CA). After centrifuging at 2000g for 5 min at 4°C, 130  $\mu\text{L}$  of MAS buffer containing cytochrome c (10  $\mu\text{g}/\text{mL}$ ) and alamethicin (10  $\mu\text{g}/\text{mL}$ ) was added to each well. The sensor cartridge plate (Agilent Technologies, Inc., Santa Clara, CA) was loaded with substrates and inhibitors (50  $\mu\text{L}$  per port) as follows: port A, NADH (1 mM) or succinate + rotenone (5 mM + 2  $\mu\text{M}$ ); port B, antimycin A (4  $\mu\text{M}$ ); port C, tetramethyl-p-phenylenediamine dihydrochloride (TMPD) + ascorbic acid (0.5 mM + 1 mM); port D, sodium azide (50 mM). All samples were run in duplicate.

### Statistical analysis

To compare mitochondrial content in brain tissues between patients with FXTAS and controls and NDEV characteristics (concentration and average size) derived by NTA between PM carriers and controls we used Mann–Whitney *U* tests. For brain tissues, we normalized mitochondrial measures by the mitochondrial content of each sample. To assess differences between the two groups (FXTAS patients and controls), we fitted linear mixed models with tissue type (frontal cortex or cerebellum), group, and tissue type-by-group interaction as fixed effects, participant as a random effect, and age as a covariate. To assess differences of mitochondrial measures in NDEVs between the two groups (PM carriers and controls), a general linear model was used with NDEV concentration as a covariate and group as a fixed effect factor. The inclusion of NDEV concentration (determined by NTA) as a covariate enabled normalization for differential NDEV yield across samples. *p* value < 0.05 was

**Figure 1.** Analysis of postmortem brain tissues of patients with FXTAS. (A, B) Comparison of the mean quantity and activity of mitochondrial complex IV in the frontal cortex (A) and cerebellum (B) of patients with FXTAS and controls. (C, D) Comparison of the mean quantity and activity of mitochondrial complex V in the frontal cortex (C) and cerebellum (D) of patients with FXTAS and controls. (E) Total mitochondrial contents in tissue lysates (20  $\mu\text{g}$  of total protein) of patients with FXTAS and controls were determined using a mitochondrial membrane-specific dye MTDR. (F) (top) Immunoblots of mitochondrial citrate synthase and Actin in cerebellum tissues; (bottom) Histogram of citrate synthase levels (normalized to Actin of the same sample) in the cerebellum of seven patients with FXTAS (f1-7) and seven controls (c1-7). Values in (A–D) were normalized by mitochondrial content of each tissue sample. Shown in each bar is mean  $\pm$  SEM. Each diamond represents data from one subject (frontal cortex, *n* = 8 for patients with FXTAS, *n* = 7 for controls; cerebellum, *n* = 8 for patients with FXTAS, *n* = 9 for controls). *p* values were calculated using Mann–Whitney *U* tests for mitochondrial contents and linear mixed models for mitochondrial measures. AU, arbitrary units; CS, citrate synthase; FXTAS, Fragile X-associated tremor/ataxia syndrome; MTDR, MitoTracker Deep Red; RFU, relative fluorescence units; \**p* < 0.05; \*\**p* < 0.01.





considered statistically significant. All analyses were performed using SPSS statistical software, version 21.0 (IBM Corp) and GraphPad Prism, version 9.0.

## Results

### Mitochondrial complex IV and complex V in brain tissues of patients with FXTAS

For Complex IV quantity and activity, the frontal cortex did not show any significant differences between patients with FXTAS and controls (Fig. 1A). In contrast, the cerebellum showed significantly reduced quantity of Complex IV in patients with FXTAS, to a level approximately 25% of controls (Fig. 1B;  $2.99 \pm 0.79$  vs.  $12.4 \pm 4.25$  AU,  $p = 0.005$ ). Moreover, the activity of complex IV in patients with FXTAS was also reduced to a level approximately 40% of controls (Fig. 1B;  $0.296 \pm 0.054$  vs.  $0.71 \pm 0.269$  AU,  $p = 0.013$ ).

Similarly, Complex V quantity and activity in the frontal cortex did not exhibit any statistically significant differences between the two groups (Fig. 1C); however, in the cerebellum, its quantity in patients with FXTAS was approximately 44% and its activity 58% lower compared to controls (Fig. 1D;  $10.9 \pm 1.92$  vs.  $24.5 \pm 7.47$  AU,  $p = 0.037$  and  $0.0189 \pm 0.0039$  vs.  $0.0324 \pm 0.0171$  AU,  $p = 0.046$ , respectively).

The assessment of total mitochondrial content in the brain tissue homogenates of patients with FXTAS and controls using the MTD method showed similar relative fluorescence intensity units between the two groups for both frontal cortex and cerebellum (Fig. 1E). Given that reductions of Complex IV and Complex V were observed solely in the cerebellum, we measured in cerebellar tissues the level of citrate synthase as an additional indicator of total mitochondrial content. Immunoblotting of citrate synthase did not show significant differences between the cerebellum of patients with FXTAS and controls (Fig. 1F). Therefore, the reduction of Complex IV and Complex V in the cerebellum of patients with FXTAS is not merely a reflection of mitochondrial loss. Collectively, our results indicate that in advanced FXTAS stages mitochondrial Complex IV and Complex V are clearly impaired in cerebellum, but not in frontal cortex, and that at least in these two brain areas, total mitochondrial content does not change significantly.

### Mitochondrial complex I and complex II respiration in brain tissues of FXTAS

For Complex I-mediated OCR (Fig. 2A), neither frontal cortex nor cerebellum of patients with FXTAS showed any differences compared to controls (Fig. 2B). Similarly,

for Complex II-mediated OCR (Fig. 2C), no differences were detected between the two groups in either brain region (Fig. 2D). Therefore, unlike the observed decreased activity of Complexes IV and V in the cerebellum of patients with FXTAS, electron transport chain activity via Complexes I and II did not appear to be severely affected.

### Mitochondrial complex IV and complex V in NDEVs of PM carriers

For NDEV-associated Complex IV quantity, we did not observe any differences between PM carriers and controls (Fig. 3A, left; mean  $\pm$  standard error (SEM)  $4.52 \pm 0.54$  vs.  $3.65 \pm 0.37$  AU,  $p = 0.46$ ). On the other hand, the NDEV-associated Complex IV activity was approximately 60% lower in PM carriers compared to controls (Fig. 3A, right;  $26.5 \pm 4.16$  vs.  $45.9 \pm 3.43$  AU,  $p = 0.02$ ).

For NDEV-associated Complex V, we found that its quantity was increased in PM carriers compared to controls (Fig. 3B, left;  $2.44 \pm 0.18$  vs.  $1.59 \pm 0.19$  AU,  $p = 0.03$ ). Despite the noticeably greater quantity, the activity of NDEV-associated Complex V in PM carriers was lower compared to controls (Fig. 3B, right;  $36.7 \pm 4.67$  vs.  $61.8 \pm 13.4$  AU,  $p = 0.046$ ).

To determine whether the changes in NDEV-associated Complex IV and Complex V in PM carriers were due to differences in the concentration of recovered NDEVs, NTA was performed, as previously done in NDEV biomarker studies.<sup>34</sup> NTA showed that NDEV diameter ranged from 85 to 180 nm, consistent with a mixed population of small and large EVs.<sup>35</sup> Comparing the NDEVs of PM carriers to those of controls, we did not observe any differences in either the number or the average diameter of the NDEVs (Fig. 3C). We conclude that the NDEVs of PM carriers contain abnormal mitochondrial Complex IV and Complex V, potentially reflecting similar abnormalities in brain neurons that generated these NDEVs.

## Discussion

Previous studies of blood samples and skin-derived fibroblasts of *FMR1* PM carriers with and without FXTAS have shown abnormal mitochondria, implying a defective machinery for oxidative phosphorylation and possibly ATP production in examined tissues and cells that ostensibly also pertain to the brain.<sup>11–15</sup> However, different organs and cells have distinctively different capacities for mitochondrial ATP production because the demands for ATP are tissue- and cell-specific.<sup>36–39</sup> Therefore, the question remaining to be answered is to what extent the mitochondrial functional status of the periphery echoes that of the brain—especially, in brain areas affected by FXTAS.

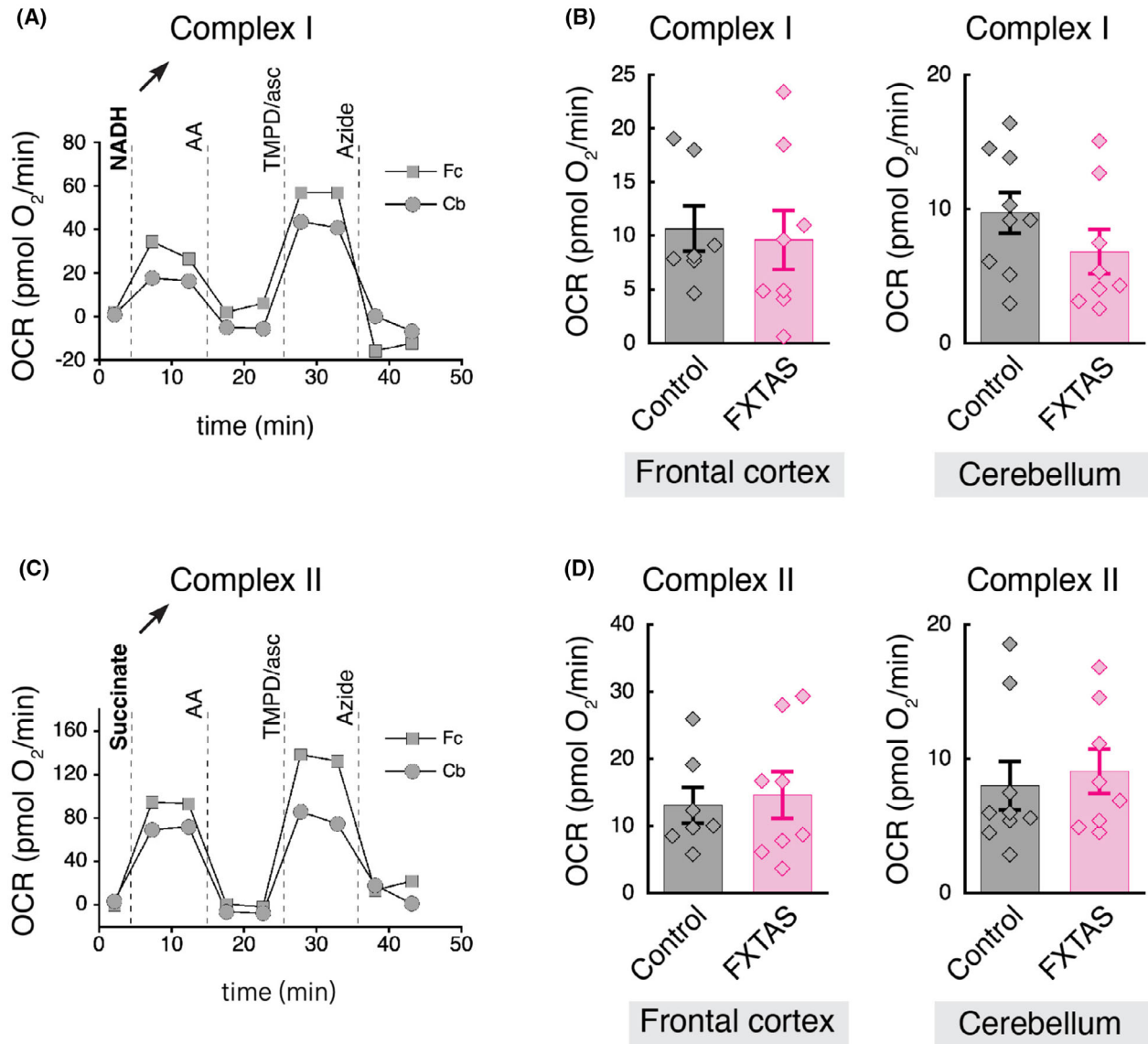
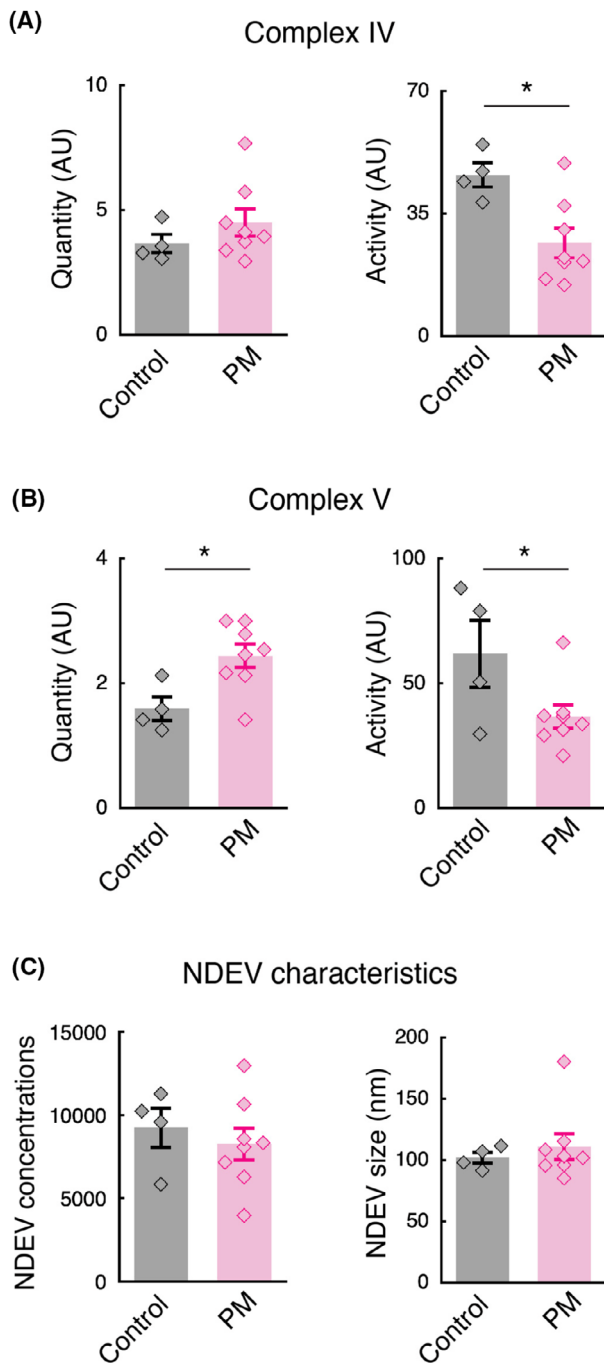


**Figure 2.** Analysis of mitochondrial complex I- and complex II-mediated respiration in brain tissues of patients with FXTAS. (A) Example traces of NADH-induced respiration representing Complex I-mediated OCR of frozen frontal cortex and cerebellum homogenates from control subjects. (B) Comparison of Complex I-mediated OCR in the frontal cortex and cerebellar tissues from patients with FXTAS and controls. (C) Example traces of succinate-induced respiration representing Complex II-mediated OCR of frozen frontal cortex and cerebellum homogenates from control subjects. (D) Comparison of Complex II-mediated OCR in the frontal cortex and cerebellar tissues from patients with FXTAS and controls. In (B) and (D), shown in each bar is mean  $\pm$  SEM. Each diamond represents data from one subject (frontal cortex,  $n = 8$  for patients with FXTAS,  $n = 7$  for controls; cerebellum,  $n = 8$  for patients with FXTAS,  $n = 9$  for controls). Analysis was performed by fitting linear mixed models. AA, antimycin A; Asc, ascorbic acid; Cb, cerebellum; Fc, frontal cortex; FXTAS, Fragile X-associated tremor/ataxia syndrome; NADH, nicotinamide adenine dinucleotide hydrogen; OCR, oxygen consumption rate; TMPD, tetramethyl-p-phenylenediamine dihydrochloride.

In this study, we investigated the mitochondrial oxidative phosphorylation proteins in postmortem brain tissues of patients with FXTAS. We found severely impaired mitochondrial Complex IV and Complex V in the cerebellum of patients with FXTAS, but not in the frontal cortex (Fig. 1B,D), consistent with the predominantly

cerebellar manifestations of the syndrome. However, not all mitochondrial parameters showed detectable alterations. For example, in both the cerebellum and the frontal cortex, total mitochondrial contents (Fig. 1E,F) and mitochondrial integrated respiration capacity driven by Complexes I and II (Fig. 2B,D) did not differ between





patients with FXTAS and controls. These findings suggest that the mitochondrial defects might be specific to the Complexes IV and V of the oxidative phosphorylation machinery. Therefore, the subsequent study in NDEVs focused on mitochondrial Complexes IV and V, which were both found impaired in PM carriers, with their activity levels being approximately 60% lower than those of controls (Fig. 3A,B).

**Figure 3.** Analysis of plasma NDEVs of premutation (PM) carriers. (A) Comparison of the mean quantity and activity of mitochondrial respiratory chain complex IV in NDEVs of PM carriers and control subjects. (B) Comparison of the mean quantity and activity of mitochondrial respiratory chain complex V in NDEVs of PM carriers and control subjects. (C) Comparison of the concentration (particles/ $\mu\text{L}$ ) and average diameter of NDEVs between PM carriers and control subjects. Shown in each bar is mean  $\pm$  SEM. Each diamond represents data from one subject ( $n = 8$  for PM carriers,  $n = 4$  for control subjects).  $p$  values were calculated using Mann–Whitney  $U$  tests for NDEV characteristics and a general linear model for mitochondrial measures. AU, arbitrary units; PM, premutation;  $*p < 0.05$ .

Based on these findings, our study highlights an important pathogenic mechanism in FXTAS, and specifically implicates Complexes IV and V, whose combined defects may lead to decreased ATP production (creating an energy crisis for neurons) and a situation where electrons are not propagated all the way across the electron transport chain to create molecules of water, but instead may become available for the formation of reactive oxygen species. Additionally, our results suggest that the quantitative and functional abnormalities observed in plasma NDEVs may be an early reflection of defects in the mitochondrial function of cerebellar neurons that are already established at the PM carrier stage before symptoms appear. Finally, our study provides potential targets for treatment with therapeutic agents that would restore the mitochondrial oxidative phosphorylation abnormalities. For example, sulforaphane, a natural phytochemical activating the nuclear factor erythroid 2-related factor (Nrf-2) that upregulates antioxidant response elements to counteract oxidative stress damage due to mitochondrial dysfunction,<sup>40</sup> has shown beneficial effects in patients with FXTAS and is under investigation.<sup>41</sup>

Nevertheless, limitations of our study need to be recognized. Despite the overall congruency of results between cerebellar tissues and NDEVs, the quantity of Complex V was found decreased in the former and increased in the latter compared to controls. A possible explanation for this discrepancy may be that, as NDEVs are derived from neurons in multiple brain regions, their protein cargo can be expected to reflect the average of neuronal homeostatic status, and not the cerebellar neuronal specific status. Additionally, although we jointly discuss results from brain tissues and NDEVs to draw conclusions, these were derived from different cohorts at different stages of the pathologic continuum (preclinical vs. advanced disease), while also the sample size was small. Finally, due to the limited volumes of plasma samples and the finite amounts of proteins in EVs, we were only able to conduct a limited number of mitochondrial assays. Further validation of our results is warranted with large longitudinal cohorts including *FMRI*

PM carriers before and after the development of FXTAS, but also with mechanistic studies that would investigate in-depth the defects in mitochondrial oxidative phosphorylation proteins and their consequences.

## Acknowledgments

This research was supported in part by the Intramural Research Program of the National Institute on Aging, NIH, and by the NIH grants RO1HD036071, NS107131, R01NS110100.

## Author Contributions

Conception and design of the study, acquisition of data, drafting the manuscript and figures: Pamela J. Yao. Analysis of data and drafting the manuscript: Apostolos Manolopoulos. Analysis of data and review of the manuscript: Erden Eren. Acquisition of data and review of the manuscript: Susan Michelle Rivera. Acquisition of data and review of the manuscript: David R. Hessel. Acquisition of data and review of the manuscript: Randi Hagerman. Acquisition of data and review of the manuscript: Veronica Martinez-Cerdeno. Conception and design of the study, acquisition of data and review of the manuscript: Flora Tassone. Conception and design of the study, analysis of data, and review of the manuscript: Dimitrios Kapogiannis.

## Conflict of Interest Statement

The authors have no conflict of interests to declare.

## Data Availability Statement

The raw data containing EV biomarker measurements and supporting the conclusion of this article will be provided to any interested investigators upon request and without undue reservation via email. Data will be de-identified prior to being shared.

## References

- Bourgeois JA, Cogswell JB, Hessel D, et al. Cognitive, anxiety and mood disorders in the fragile X-associated tremor/ataxia syndrome. *Gen Hosp Psychiatry*. 2007;29(4):349-356.
- Filley CM, Brown MS, Onderko K, et al. White matter disease and cognitive impairment in FMR1 premutation carriers. *Neurology*. 2015;84(21):2146-2152.
- Hagerman RJ, Leehey M, Heinrichs W, et al. Intention tremor, parkinsonism, and generalized brain atrophy in male carriers of fragile X. *Neurology*. 2001;57(1):127-130.
- Salcedo-Arellano MJ, Wolf-Ochoa MW, Hong T, et al. Parkinsonism versus concomitant Parkinson's disease in fragile X-associated tremor/ataxia syndrome. *Mov Disord Clin Pract*. 2020;7(4):413-418.
- Hagerman RJ, Hagerman P. Fragile X-associated tremor/ataxia syndrome - features, mechanisms and management. *Nat Rev Neurol*. 2016;12(7):403-412.
- Jacquemont S, Hagerman RJ, Hagerman PJ, Leehey MA. Fragile-X syndrome and fragile X-associated tremor/ataxia syndrome: two faces of FMR1. *Lancet Neurol*. 2007;6(1):45-55.
- Greco CM, Berman RF, Martin RM, et al. Neuropathology of fragile X-associated tremor/ataxia syndrome (FXTAS). *Brain*. 2006;129(Pt 1):243-255.
- Greco CM, Hagerman RJ, Tassone F, et al. Neuronal intranuclear inclusions in a new cerebellar tremor/ataxia syndrome among fragile X carriers. *Brain*. 2002;125(Pt 8):1760-1771.
- Tassone F, Hagerman RJ, Garcia-Arocena D, Khandjian EW, Greco CM, Hagerman PJ. Intranuclear inclusions in neural cells with premutation alleles in fragile X associated tremor/ataxia syndrome. *J Med Genet*. 2004;41(4):e43.
- Ross-Inta C, Omanska-Klusek A, Wong S, et al. Evidence of mitochondrial dysfunction in fragile X-associated tremor/ataxia syndrome. *Biochem J*. 2010;429(3):545-552.
- Giulivi C, Napoli E, Tassone F, Halmai J, Hagerman R. Plasma biomarkers for monitoring brain pathophysiology in FMR1 Premutation carriers. *Front Mol Neurosci*. 2016;9:71.
- Loesch DZ, Godler DE, Evans A, et al. Evidence for the toxicity of bidirectional transcripts and mitochondrial dysfunction in blood associated with small CGG expansions in the FMR1 gene in patients with parkinsonism. *Genet Med*. 2011;13(5):392-399.
- Napoli E, Ross-Inta C, Wong S, et al. Altered zinc transport disrupts mitochondrial protein processing/import in fragile X-associated tremor/ataxia syndrome. *Hum Mol Genet*. 2011;20(15):3079-3092.
- Napoli E, Song G, Schneider A, et al. Warburg effect linked to cognitive-executive deficits in FMR1 premutation. *FASEB J*. 2016;30(10):3334-3351.
- Napoli E, Song G, Wong S, Hagerman R, Giulivi C. Altered bioenergetics in primary dermal fibroblasts from adult carriers of the FMR1 premutation before the onset of the neurodegenerative disease fragile X-associated tremor/ataxia syndrome. *Cerebellum*. 2016;15(5):552-564.
- van Niel G, D'Angelo G, Raposo G. Shedding light on the cell biology of extracellular vesicles. *Nat Rev Mol Cell Biol*. 2018;19(4):213-228.
- Dickens AM, Tovar YRLB, Yoo SW, et al. Astrocyte-shed extracellular vesicles regulate the peripheral leukocyte response to inflammatory brain lesions. *Sci Signal*. 2017;10(473).
- Mustapic M, Eitan E, Werner JK Jr, et al. Plasma extracellular vesicles enriched for neuronal origin: a

- potential window into brain pathologic processes. *Front Neurosci.* 2017;11:278.
19. Yao PJ, Eren E, Goetzl EJ, Kapogiannis D. Mitochondrial electron transport chain protein abnormalities detected in plasma extracellular vesicles in Alzheimer's disease. *Biomedicine.* 2021;9(11).
  20. Ladakis DC, Yao PJ, Vreones M, et al. Mitochondrial measures in neuronally enriched extracellular vesicles predict brain and retinal atrophy in multiple sclerosis. *Mult Scler.* 2022;28(13):2020-2026.
  21. Blommer J, Pitcher T, Mustapic M, et al. Extracellular vesicle biomarkers for cognitive impairment in Parkinson's disease. *Brain.* 2023;146(1):195-208.
  22. Bhargava P, Nogueras-Ortiz C, Kim S, Delgado-Peraza F, Calabresi PA, Kapogiannis D. Synaptic and complement markers in extracellular vesicles in multiple sclerosis. *Mult Scler.* 2021;27(4):509-518.
  23. Vandendriessche C, Kapogiannis D, Vandenbroucke RE. Biomarker and therapeutic potential of peripheral extracellular vesicles in Alzheimer's disease. *Adv Drug Deliv Rev.* 2022;190:114486.
  24. Giulivi C, Wang JY, Hagerman RJ. Artificial neural network applied to fragile X-associated tremor/ataxia syndrome stage diagnosis based on peripheral mitochondrial bioenergetics and brain imaging outcomes. *Sci Rep.* 2022;12(1):21382.
  25. Vilcaes AA, Chanaday NL, Kavalali ET. Interneuronal exchange and functional integration of synaptobrevin via extracellular vesicles. *Neuron.* 2021;109(6):971-983 e5.
  26. D'Acunzo P, Perez-Gonzalez R, Kim Y, et al. Mitovesicles are a novel population of extracellular vesicles of mitochondrial origin altered in down syndrome. *Sci Adv.* 2021;7(7).
  27. Dufour BD, Albores-Gallo L, Luna-Munoz J, et al. Hispano-American brain Bank on neurodevelopmental disorders: an initiative to promote brain banking, research, education, and outreach in the field of neurodevelopmental disorders. *Brain Pathol.* 2022;32(2): e13019.
  28. Jacquemont S, Hagerman RJ, Leehey M, et al. Fragile X premutation tremor/ataxia syndrome: molecular, clinical, and neuroimaging correlates. *Am J Hum Genet.* 2003;72(4):869-878.
  29. Hall DA, Birch RC, Anheim M, et al. Emerging topics in FXTAS. *J Neurodev Disord.* 2014;6(1):31.
  30. Cottet-Rousselle C, Ronot X, Leverve X, Mayol JF. Cytometric assessment of mitochondria using fluorescent probes. *Cytometry A.* 2011;79(6):405-425.
  31. Yao PJ, Munk R, Gorospe M, Kapogiannis D. Analysis of mitochondrial respiration and ATP synthase in frozen brain tissues. *Heliyon.* 2023;9(3):e13888.
  32. Osto C, Benador IY, Ngo J, et al. Measuring mitochondrial respiration in previously frozen biological samples. *Curr Protoc Cell Biol.* 2020;89(1):e116.
  33. Acin-Perez R, Benador IY, Petcherski A, et al. A novel approach to measure mitochondrial respiration in frozen biological samples. *EMBO J.* 2020;39(13):e104073.
  34. Kapogiannis D, Mustapic M, Shardell MD, et al. Association of extracellular vesicle biomarkers with Alzheimer disease in the Baltimore longitudinal study of aging. *JAMA Neurol.* 2019;76(11):1340-1351.
  35. Kowal J, Arras G, Colombo M, et al. Proteomic comparison defines novel markers to characterize heterogeneous populations of extracellular vesicle subtypes. *Proc Natl Acad Sci USA.* 2016;113(8):E968-E977.
  36. Benard G, Faustin B, Passerieux E, et al. Physiological diversity of mitochondrial oxidative phosphorylation. *Am J Physiol Cell Physiol.* 2006;291(6):C1172-C1182.
  37. Fernandez-Vizarrá E, Enriquez JA, Perez-Martos A, Montoya J, Fernandez-Silva P. Tissue-specific differences in mitochondrial activity and biogenesis. *Mitochondrion.* 2011;11(1):207-213.
  38. Mootha VK, Bunkenborg J, Olsen JV, et al. Integrated analysis of protein composition, tissue diversity, and gene regulation in mouse mitochondria. *Cell.* 2003;115(5):629-640.
  39. Hansen FM, Kremer LS, Karayel O, et al. Mitochondrial phosphoproteomes are functionally specialized across tissues. *Life Sci Alliance.* 2024;7(2):e202302147.
  40. Napoli E, Flores A, Mansuri Y, Hagerman RJ, Giulivi C. Sulforaphane improves mitochondrial metabolism in fibroblasts from patients with fragile X-associated tremor and ataxia syndrome. *Neurobiol Dis.* 2021;157:105427.
  41. Santos E, Clark C, Biag HMB, et al. Open-label sulforaphane trial in FMR1 premutation carriers with fragile-X-associated tremor and ataxia syndrome (FXTAS). *Cells.* 2023;12(24).